Thermoelasticity and interdiffusion in CuNi multilayers

M. C. Benoudia, F. Gao, J.-M. Roussel,* S. Labat, M. Gailhanou, and O. Thomas
IM2NP, UMR 6242 CNRS, Université Aix-Marseille, Faculté des Sciences et Techniques de Saint-Jérôme, Service 262, F-13397 Marseille Cedex 20, France

D. L. Beke, Z. Erdélyi, and G. Langer
Department of Solid State Physics, University of Debrecen, H-4010 Debrecen, P.O. Box 2, Hungary

A. Csik and M. Kis-Varga
Institute of Nuclear Research of the Hungarian Academy of Sciences, H-4001 Debrecen, P.O. Box 51, Hungary
(Received 1 March 2012; published 4 June 2012)

X-ray scattering experiments on coherent CuNi multilayers are performed at various annealing temperatures. First, we show that the classical thermoelasticity theory can be applied in such nanosamples to link composition and strain fields at intermediate temperature. Second, when interdiffusion takes place at higher temperature, the satellite peaks measured at different annealing times indicate the presence of a layer-by-layer interdiffusion mode controlled by the asymmetry of the atomic mobilities in this system.

DOI: 10.1103/PhysRevB.85.235404 PACS number(s): 68.35.Fx, 62.25.−g, 68.65.Ac, 61.05.cp

I. INTRODUCTION

The idea of observing artificial metallic multilayers with x-ray diffraction techniques to study interdiffusion phenomena dates back to the work of DuMond and Youtz.[1,2] Interestingly, these pioneering contributions even suggested that the approach could be used to measure the concentration dependence of the diffusion coefficient.[2] This remark is precisely the subject of the present work: we aim to revisit this issue in light of recent atomistic simulation results obtained for coherent CuNi multilayers.[3]

More generally, CuNi multilayers have been extensively studied for their magnetic, mechanical, and optical properties.[4–9] These physical properties depend critically on interfaces and require a good control on the evolution of composition and strain fields under heat treatment. Understanding of how interdiffusion proceeds in these nanosystems should therefore improve these practical aspects. From a theoretical viewpoint these synthetic modulated structures have been also used as valuable model systems to test the various diffusion theories accounting in particular for the influence of the alloying energy, the coherency strain, and the local concentration.[5,10] Nowadays, this field remains active and has been extended with the development of atomic simulations and many microscopy techniques like atom probe tomography which give details on the intermixing mechanisms.[11,12]

As mentioned, the starting point of the present x-ray diffraction study comes from recent atomistic simulation results obtained for coherent CuNi multilayers. It is found that an unusual layer-by-layer interdiffusion mode should take place in such systems even though Cu and Ni elements are highly miscible.[3] This particular interdiffusion mode, which was known for phase separation film/substrate systems,[13–15] is in the case of the CuNi system the result of a strong asymmetry of the atomic mobilities or, in other words, due to a marked concentration dependence of the diffusion coefficient.[3,16,17] During interdiffusion, the initial Ni pure regions should decrease in size but remain almost pure in composition while the initial Cu pure regions are progressively enriched in Ni diluted atoms forming a solid solution with an increasing concentration. How can such a phenomenon be evidenced from x-ray scattering experiments? In principle, this nondestructive technique provides the pertinent quantities (angular shift, peak intensities) which are sensitive to the composition and the strain field.[6,18–21] However, the analysis of the x-ray diffractograms giving access to both the lattice strain and, more importantly here, to the chemical composition requires a realistic model that links the two profiles together. In the presence of coherent interfaces this model will constrain the search of the physical solution in composition and strain. In the first section of this paper, using the temperature dependence of the elastic constants and the lattice parameters in the CuNi system, we first verify experimentally that, even for a stacking of bilayers having a thickness of 6 nanometers, the change of the x-ray diffractogram with the temperature is consistent with a model based on the classical elasticity theory. This modeling gives, in the second section, the framework to interpret our experiments performed at higher temperatures where irreversible intermixing takes place. Perspectives and conclusions of this work are given in the last section.

II. THERMOELASTICITY

The presence of grain boundaries or dislocation leads to short circuit diffusion paths and also to complicated thermoelastic behaviors that we wish to avoid in the present study. Ideally, to focus on the role of bulk interdiffusion, the CuNi multilayer should have coherent interfaces and approach a single crystal. In this case, the interdiffusion is mainly mediated by a vacancy jump mechanism and the multilayer obeys a clear thermoelastic behavior that simplifies the analysis of the resulting diffractograms. For this point, it is often assumed that classical elasticity theory describes properly the relation between strain and composition in these coherent multilayers. In other words, from the elementary bulk properties of the two elements forming the mutlilayer (i.e., lattice parameters, elastic constants), the resulting x-ray

diffractograms can be seen as a macroscopic coherent system under biaxial strain. Thus, one can easily quantify (at least for planar sharp interfaces) the total number of bilayers, their composition, their fluctuation in size, and the interplane distances in the Cu-rich and the Ni-rich regions. Recent atomistic simulations agree with this picture by pointing out, however, that due to interfacial relaxation effects, some deviations from the classical modeling should appear with an impact on the diffractogram in the case of short composition wavelengths.[22] At the other extreme for large bilayers, it is well known that a model based on elasticity theory will become unsuitable when misfit dislocations appear to relieve the strain energy. Besides, once this loss of coherency occurs, the kinetics of interdiffusion should certainly deviate from a pure bulk interdiffusion driven by a variation of composition only.

In this section, the samples are made of 25 $[Cu_{2.48nm}Ni_{3.75nm}]$ bilayers synthesized at 473 K by magnetron sputtering on a (001) MgO substrate. We first detail the properties of the samples found at room temperature. We measure the d spacings of the planes perpendicular to the film by grazing x-ray diffraction. In addition to the 200 MgO peak, a single 200 reflection is observed [see the inset in Fig. 1(a)] between the positions expected for the 200 reflections of pure Cu and pure Ni. This result shows that the interfaces are coherent. The in-plane distance $d_{\parallel} = d_{200}$ shared by both the Cu and Ni regions is found to be very close to the average $d_{\parallel} = (d_{200}^{Cu} + d_{200}^{Ni})/2$ where d_{200}^{Cu} and d_{200}^{Ni} are the bulk equilibrium values. Note that the $d_{\parallel}$ in the multilayer is different from the one in the substrate, meaning that the multilayer does not match with the substrate.

From the rocking curve performed on the MgO substrate (not shown here), we learn that the MgO crystal is formed by a few subgrains with a low misorientation of 0.05° between them. The rocking curves obtained on the Cu/Ni multilayer exhibit 002 and 004 peaks from the Cu/Ni multilayer have the same width (about 2.15° at half maximum) indicating, in the frame of a mosaic bloc model, that this texture is essentially a misorientation mosaicity.[23] Figures 1(a) and 1(b) show parts of the out-of-plane x-ray diffraction pattern (first and second orders peaks) obtained as a function of the scattering vector **q** parallel to the growth direction. The modulation in intensity is typical of a multilayer. The numerous peaks originate from the periodic stacking of Ni/Cu bilayers. The position of the main I_0 peak in Fig. 1(a), corresponds to the average out-of-plane d spacing. The other satellite peaks are labeled as indicated in the figure. Note that in the whole out-of-plane diffraction pattern along this scattering vector **q** (not shown here) we observe the 002 and 004 peaks corresponding to the MgO substrate. This means that both the substrate and the multilayer have the same (001) crystal orientation.

From Fig. 1, we now proceed to the classical analysis of such curves to extract the pertinent quantities. The as-grown multilayer ends with a free (001) surface. The sample is therefore free of stress in this direction z. Besides the multilayer is coherent and the Ni and Cu layers undergo an elastic strain. From the $d_{\parallel}$ value observed here, the Cu element with the larger lattice parameter is compressed while the Ni layers are under tension. In this geometry, the coherency strain causes a contraction (or, respectively, a dilatation) of the

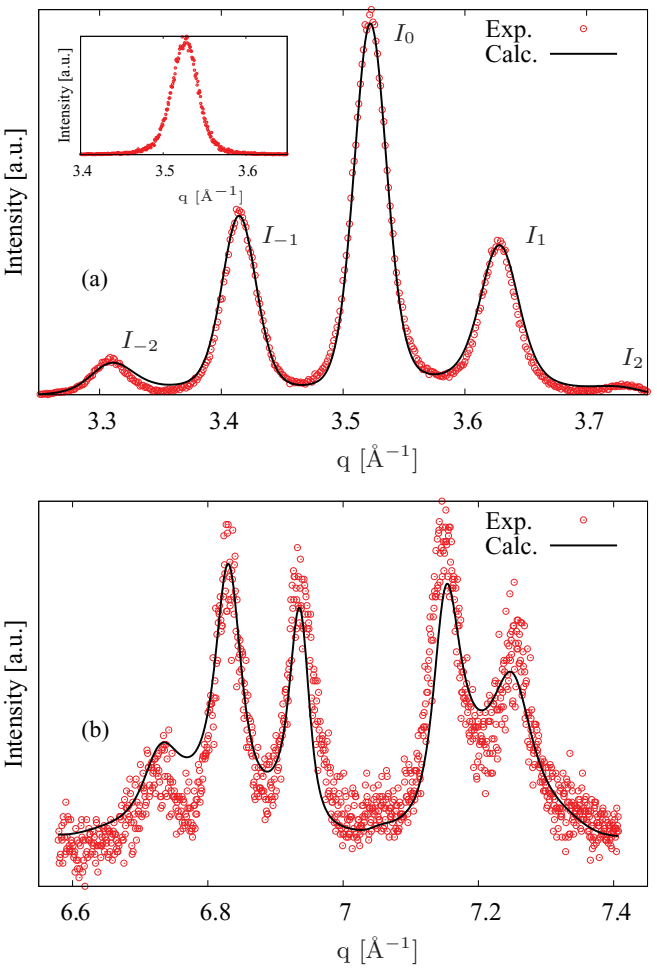

FIG. 1. (Color online) Experimental (circle) and calculated (thick line) out-of-plane x-ray diffractogram (a) first order 002 and (b) second order 004 from a CuNi 25 $[Cu_{2.48nm}Ni_{3.75nm}]$ bilayers at 298 K. In-plane 200 measurement is shown in the inset.

interplane distances $d_{\perp}(z)$ along the z axis perpendicular to the interface if these planes contain the smallest element (nickel atoms) or, respectively, the biggest element (copper atoms). For pure planes that are relatively away from the interfaces the values of the $d_{\perp}(z)$ spacings can be evaluated from the classical elasticity theory. Using Voigt notation for a cubic system with a coordinate axis taken to be the principal axis and considering that the principal stresses σ_i and strains ϵ_i obey a state of biaxial stress we have $\sigma_1 = \sigma_2 = \sigma$ and $\sigma_3 = \sigma_4 = \sigma_5 = \sigma_6 = 0$. This tetragonal distortion also implies that $\epsilon_1 = \epsilon_2 = \epsilon_{\parallel} = d_{\parallel}/d_0 - 1$ and $\epsilon_3 = \epsilon_{\perp} = d_{\perp}/d_0 - 1$, where $d_0 = a_0/2$ is the bulk equilibrium interplane distance. Using the linear relationship $\sigma_i = C_{ij}\epsilon_j$ between stress and strain through the elastic constants C_{ij}, one obtains

$$\epsilon_{\perp} = \frac{-2C_{12}}{C_{11}}\epsilon_{\parallel}, \tag{1}$$

and therefore a direct estimation of the resulting $d_{\perp}(z)$ interplane distances in z pure regions.

Considering now a region where along z the concentration $c(z)$ varies smoothly, one can also use Eq. (1) to estimate the interplane distance $d_{\perp}[c(z)]$ by taking into account the fact that both elastic constants and the equilibrium lattice parameter

$a_0 = 2d_0$ of the solid solution change with c. In the present work, we use a linear variation with c of the quantities $d_0(c)$, $C_{12}(c)$, and $C_{11}(c)$ leading to a simple polynomial form of the expression of $d_\perp[c(z)]$. These simple approximations mimic well the bulk properties of the CuNi system.[24–27] In practice, on a discrete lattice where concentration c_j is defined per plane j, the spacing between two adjacent planes j and $j+1$ is evaluated from Eq. (1) by replacing $c(z)$ with the average value $[c_j + c_{j+1}]/2$. Let us note, however, that there are some limitations of the above model [Eq. (1)] that were quantified in a previous work based on atomistic calculations.[22] Due to the interfacial relaxations found in the CuNi system, the $d_\perp$ profile should also depend on the local concentration gradient. It is shown, however, that this effect is not measurable from the first order satellite peaks $I_{\pm1}$ and $I_{\pm2}$ on the present x-ray diffractograms. Such interfacial phenomena will affect significantly the x-ray scattered intensity for CuNi multilayers having shorter composition modulation length (roughly three times smaller).

From Eq. (1) one gets the z positions z_j of all the j atomic planes. Considering sharp chemical interfaces between pure Ni and Cu regions, the calculations of the x-ray diffraction spectra are made in the framework of the kinematic theory in the simple Bragg geometry where the scattering vector $\mathbf{q}$ is parallel to the z direction. The x-ray scattered intensity $I(q)$ of one multilayer containing N identical bilayers can be evaluated from the product:[18] $I(q) \propto |S(q)|^2|F(q)|^2$ where $S(q) = \sin(Nq\lambda\bar{d}/2)/\sin(q\lambda\bar{d}/2)$ is the interference function of the superlattice with $\bar{d}$ defined as the average interplane distance, λ the number of planes in the bilayer, and $F(q)$ is the structure factor of the bilayer that is calculated by summing over all the j planes $F(q) = \sum_j f_j(q)\exp(-iqz_j)$ with $f_j(q) = c_j f_{\mathrm{Ni}}(q) + (1-c_j) f_{\mathrm{Cu}}(q)$ being the scattering factor of the jth planes. The expressions and values of the complex atomic scattering factor $f_{\mathrm{Ni}}(q)$ and $f_{\mathrm{Cu}}(q)$ are taken from Refs. 28,29 at the x-ray energy corresponding to the copper emission line K_α. A Debye-Waller factor is also used as a correction of the atomic scattering factor to take into account the effect of the temperature on the diffraction curves. A rough estimation from the case of elements in the bulk environment[30] indicates that this vibrational effect is not significant (the maxima of the peaks are lowered by less than 1%) for the temperatures considered. The values of $f_{\mathrm{Ni}}(q)$ and $f_{\mathrm{Cu}}(q)$ used in this work to calculate the out-of-plane x-ray spectra are reported in Table I for $q \approx 3.5$ Å^{-1}. To account for some fluctuation in the size of the bilayers in the sample, we use the modeling chosen by Fullerton *et al.*[31] for this type of disorder. This effect of thickness fluctuations is described by assuming discrete Gaussian variations around the average values N_{Ni} and N_{Cu} of the numbers of Ni and Cu planes with two parameters σ_{Ni} and σ_{Cu} (in the number of planes) that control the respective distribution widths.[31] Finally, to mimic the additional symmetrical broadening of the experimental peaks that is caused by the limited instrumental resolution, the calculated profiles are convoluted with a Gaussian response function with a width (controlled by the parameter σ_{conv}) corresponding to the resolution of the diffractometer. We now compare in Fig. 1 the theoretical x-ray scattered intensity $I(q)$ with our measurements performed at room temperature. The good agreement between the experiments and calculations shown in Figs. 1(a) and 1(b) is obtained after the following fitting procedure. For a composition profile corresponding only to pure regions and sharp interfaces, the interplanes distances are determined from the elastic model of Eq. (1) using the measured in-plane distance $d_\parallel$ and the data reported in Table I. Thus, away from the interface, we obtain $d_\perp^{\mathrm{Ni}} = 1.739$ Å and $d_\perp^{\mathrm{Cu}} = 1.8449$ Å. Then, from the angular positions of the experimental peaks, we deduce the average number of Ni and Cu planes ($N_{\mathrm{Ni}} = 18.85$ and $N_{\mathrm{Cu}} = 13.89$) per bilayer. Finally, by accounting for the above-mentioned statistical disorder, all the peaks are broadened and high order satellite intensities are decreased. The best fit is obtained for $\sigma_{\mathrm{Ni}} = 2.1$ and $\sigma_{\mathrm{Cu}} = 2.5$ with the instrumental parameter σ_{conv} fixed to 0.18.

TABLE I. Elastic constants, bulk $d_{002} = d_0$ distance, measured in-plane $d_\parallel$ distance, values of the x-ray scattering factors f at $q \approx 3.5$ Å^{-1} for Cu and Ni elements at the various temperatures considered in this work.

	C_{11} (MPa)	C_{12} (MPa)	d_0 (Å)	$d_\parallel$ (Å)	$f(q \approx 3.5$ Å$^{-1})$
$T = 298$ K					
Cu	169	122	1.8076	1.781975	$18.09 + 0.56i$
Ni	251	150	1.7620	1.781975	$16.10 + 0.50i$
$T = 363$ K					
Cu	167	121	1.8096	1.783245	$17.94 + 0.56i$
Ni	248	150	1.7636	1.783245	$16.01 + 0.49i$
$T = 458$ K					
Cu	163	119	1.8127	1.785271	$17.72 + 0.55i$
Ni	242	149	1.7661	1.785271	$15.88 + 0.49i$
$T = 640$ K					
Cu	156	116	1.8187	1.789	$17.30 + 0.54i$
Ni	230	148	1.7710	1.789	$15.63 + 0.48i$

Having characterized the multilayer at room temperature, we can now test the composition strain model of Eq. (1) through the variation with temperature of the quantities C_{11}, C_{12}, d_0, and $d_\parallel$. For this purpose, we have performed *in situ* x-ray measurements at two annealing temperatures $T = 363$ K and $T = 458$ K. The temperature of the sample is known by measuring the MgO thermal expansion by x-ray diffraction.[32] The first order out-of-plane x-ray spectra are plotted in Fig. 2 and the values of the in-plane distances $d_\parallel$ are reported in Table I. To ensure that experiments are made in a thermoelastic regime, we verify that the diffraction curves observed at $T = 298$ K and $T = 363$ K are well recovered at these temperatures after having performed the highest temperature measurement at $T = 458$ K. Clearly, this reversibility is checked and the sample appears unchanged after this temperature cycle.

During the temperature annealing of the sample two major changes can be seen in Fig. 2. First, one observes an angular shift of the whole spectra. This shift to the left corresponds to an increase of the average perpendicular d spacing that is well reproduced by the thermoelastic model using the data of Table I (note that the in-plane d spacing $d_\parallel$ is found to increase smoothly). Second, all the satellite peak intensities increase when the temperature increases. This behavior is very different from the case where interdiffusion takes place, as i will be shown in the next section. This phenomenon is also well captured by the calculated spectra.

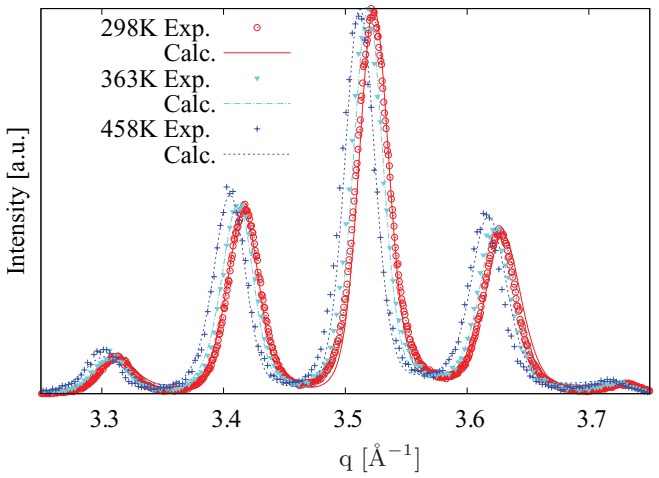

FIG. 2. (Color online) Experimental (symbols) and calculated (lines) out-of-plane x-ray diffractograms obtained at first order 002 for different temperatures ($T = 298$, 363, and 458 K) from CuNi 25 [$Cu_{2.48nm}Ni_{3.75nm}$] bilayers.

To summarize, we have shown that classical thermoelastic arguments combined with bulk data can be used to model the x-ray scattered intensity of annealed coherent CuNi multilayers. This result provides a valuable framework to analyze the evolution of the concentration profiles at higher temperature in the next section.

III. INTERDIFFUSION

The second part of this study concerns the interdiffusion mode that takes place in CuNi multilayers at higher temperature. In theory, the strong asymmetry of the atomic mobilities in this system should lead to a layer-by-layer mode where the initial Ni pure regions decrease in thickness but remain almost pure and where the initial Cu pure regions are more and more enriched by isolated Ni atoms forming a solid solution. This phenomenon is explained from pure kinetic arguments by considering the properties of the vacancies in this system. Interdiffusion is mediated by these point defects that are mainly found in the Cu-rich regions where the vacancy formation energy is lower. Vacancy jumps are also much more frequent in the Cu-rich regions. Consequently, Ni atoms are detached one by one from the interface and diffuse towards the Cu regions. The composition profile of the interface remains sharp and moves layer-by-layer to the Ni-rich regions. Interestingly, this particular interdiffusion mode can be captured by a one-dimensional kinetic mean-field model where the interdiffusion coefficient varies exponentially with the concentration. We will use this simplified description of interdiffusion to study the time variation of the x-ray scattered intensity during the interdiffusion. Since the basis of this diffusion model has been described in several articles[16,33,34] only a brief description will be given here. The diffusion is modeled by an effective exchange mechanism between atoms and, it is thus characterized by one interdiffusion coefficient D. In an $A_{1-c}B_c$ homogeneous alloy where Cu = A and Ni = B, the composition dependence of this diffusion coefficient is assumed to follow $D(c) = D(0)\exp(-mc)$, where the parameter m gives the degree of asymmetry of the diffusion coefficient. At the atomic scale, using a broken bond model, this asymmetry can also be expressed in terms of the difference between the strength of V_{AA} and V_{BB} pairwise interaction energies, $m = Z(V_{AA} - V_{BB})/kT$, where $Z = 12$ is the coordination number in the fcc structure. The second parameter of this model is the ordering energy $V_{AA} + V_{BB} - 2V_{AB}$ whose sign gives the tendency towards ordering or towards phase separation. It is taken null here since in the CuNi phase diagram phase separation is very weak [with a critical temperature around 630 K (Ref. 35)]. In the frame of this diffusion model, we have performed one-dimensional kinetic mean-field simulations by considering homogeneous concentrations per plane parallel to the interfaces. The time dependence of the concentration per plane is calculated as a detailed balance between incoming and outcoming fluxes.[33] The second parameter $D(0)$ controls the time scale of the simulations but should be consistent with both our experimental annealing time and the bulk diffusion data available on that system [i.e., $D(0) = D^{Cu}_{Ni^*} \approx 6\ 10^{-23} m^2 s^{-1}$ at 650 K (Ref. 36)]. To evaluate the asymmetry parameter m at the experimental temperature, it is possible to use the well-documented high temperature measurements available on that system. These studies performed at T = 1273 K show a strong concentration dependence of the interdiffusion coefficient D that is not strictly linear on a logscale.[37–39] Taking the two extreme values of D in pure copper $D^{Cu}_{Ni^*}$ and in pure nickel $D^{Ni}_{Cu^*}$, one obtains $m = \ln(D^{Cu}_{Ni^*}/D^{Ni}_{Cu^*}) \approx 4.6$ at 1273 K corresponding to $m \approx 9$ around 650 K. This extrapolation is also consistent with an estimation made from a previous kinetic Monte Carlo study and corresponds to a strong asymmetry of diffusion that should lead to the layer-by-layer interdiffusion mode we wish to evidence in this work.[3]

For this purpose, we consider coherent CuNi multilayers with properties similar to the one studied in Sec. II. We now discuss the case of two specific samples, denoted *sample 1* and *sample 2* for which a series of heat treatments were performed at $T = 670$ K under argon atmosphere. X-ray measurements are done *ex situ* at room temperature using the geometry and the analysis detailed in the previous section. Before annealing, satisfactory fits of the symmetrical coplanar 002 diffractograms were obtained by assuming again chemically sharp interfaces. The two samples chosen here differ mainly from their composition ratios. Numerically, we obtain the following average number of Ni and Cu planes per bilayer: $N_{Ni} = 16.45$ and $N_{Cu} = 15.05$ for *sample 1* and $N_{Ni} = 23.53$ and $N_{Cu} = 15.95$ for *sample 2*. And concerning the statistical disorder of these samples, we find $\sigma_{Ni} = 1.0$ and $\sigma_{Cu} = 2.4$ for *sample 1* and $\sigma_{Ni} = 1.4$ and $\sigma_{Cu} = 1.8$ for *sample 2*. In Fig. 3, we report all the in-plane and out-of-plane x-ray spectra collected for *sample 1* (*ex situ* at room temperature) during more than 300 hours of heat treatment at $T = 670$ K. First, the unique peak observed from the in-plane measurements shows that the multilayers remain coherent during the kinetics. More quantitatively, from the angular shift of this peak, we find a small increase of the in-plane distance $d_{\parallel}$ from 1.7828 to 1.7892 Å while from the out-of-plane diffractogram, we get (except for the very beginning of the kinetics) a decrease of the average perpendicular distance from 1.7907 to 1.7848 Å. From this macroscopic elastic-like behavior of the multilayers during the intermixing kinetics, it is difficult to extract any information on the interdiffusion mode taking place.[40] Besides, one can

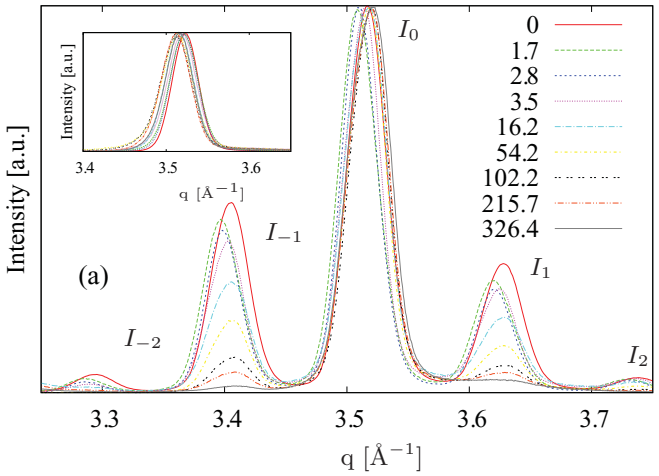

FIG. 3. (Color online) First order 002 out-of-plane x-ray diffractograms measured *ex situ* at room temperature after different annealing time (in hours) at 670 K for the CuNi *sample 1* made of 25 [$Cu_{2.77nm}Ni_{2.86nm}$] bilayers. In-plane 200 measurements are shown in the inset.

show that the influence of the variation of $d_{\parallel}$ on the intensity of the satellite peaks is not significant.[41] In the following, we will consider $d_{\parallel}$ as constant, and focus on the satellite intensities instead of the angular position of the diffraction pattern. In Fig. 3 the evolution of the x-ray scattered intensity is clearly visible and differs markedly from the thermoelastic behavior discussed in the previous section. Here the effect of intermixing is to lower the satellite peaks in favor of a unique peak corresponding to the CuNi solid solution.

Using the notation recalled in Fig. 3, we plot on a logscale in Fig. 4 the time evolution of the intensity ratios of the first and second order $I_{\pm1}(t)$ and $I_{\pm2}(t)$ with respect to the intensity of the main peak $I_0(t)$. In addition to the experimental data, we also report in Fig. 4 the results of our simulations obtained by using the above-mentioned kinetic mean-field model that takes into account a possible diffusion asymmetry. For *sample 1* the best agreement is found for an asymmetry parameter $m = 8$ and a prefactor $D(0) = 1.34\ 10^{-23}\mathrm{m}^2\mathrm{s}^{-1}$ while for *sample 2*, similar values are found with $m = 7$ and $D(0) = 1.19\ 10^{-23}\mathrm{m}^2\mathrm{s}^{-1}$. Note that these solutions minimize the chi-square error function between the measured data set and the model-generated evolution of the peak intensities. Besides, these values are consistent with the bulk diffusion asymmetry we expect in a bulk CuNi alloy. To get more refined values of the parameters m and $D(0)$ (note that m is not necessarily an integer) additional samples and/or measurements should be considered in future work. However, the overall agreement obtained in the present study for two different samples is a strong indication that the interdiffusion and the composition profiles are driven by the bulk diffusion asymmetry existing in the CuNi system. The time evolution of the concentration profiles that led to such an agreement with x-ray experiments is plotted in Fig. 5. Clearly, we are in the presence of the layer-by-layer mode we wished to evidence.

To discuss this main result of the present study, we now focus on some details of the curves shown in Fig. 4. The time dependence of the first order satellite peaks $I_{\pm1}(t)/I_0(t)$ has been studied in detail by Tsakalakos *et al.* in Ref. 8 for

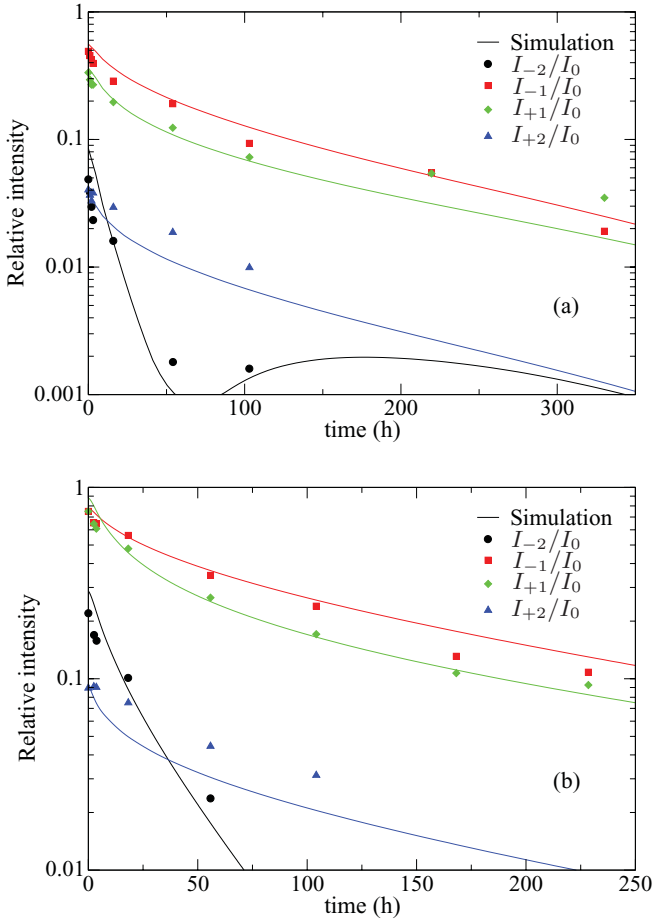

FIG. 4. (Color online) Evolution of the experimental intensities (symbols) of the satellite peak from the first order 002 out-of-plane x-ray diffractograms obtained at 670 K: (a) CuNi *sample 1* made of 25 [$Cu_{2.77nm}Ni_{2.86nm}$] bilayers and (b) CuNi *sample 2* made of 25 [$Cu_{2.94nm}Ni_{4.09nm}$] bilayers. Lines show the results of our kinetic mean-field simulations [see text].

CuNi multilayers having different composition modulation lengths. Even though in this pioneering work, $I_1(t)$ and $I_{-1}(t)$ intensities are not distinguished (the Guinier model is used, which neglects the influence of strain on the intensity of satellites), we find similar results. Both $I_1(t)/I_0(t)$ and $I_{-1}(t)/I_0(t)$ curves for *sample 1* and *sample 2* exhibit a fast decrease at the beginning of the kinetics followed by an exponential regime. To interpret this enhanced diffusivity at short time, the authors invoked different factors: recrystallization and grain growth upon annealing reducing the presence of high-diffusivity paths with time and the nonlinearity of the diffusion equation leading to nonexponential solutions at short time. Our results are in agreement with this latter conclusion. In our simulation the fast decrease observed at short time can be directly related to the nonlinearity of the equation that in our case is mainly controlled by the concentration dependence of the interdiffusion coefficient. Note, however, that the sole effect of strain field in the CuNi multilayer is to slow down the decay of $I_1(t)$ and $I_{-1}(t)$ at short time (i.e., contrary to the diffusion asymmetry effect). This is shown in the simulations when diffusion asymmetry is switched off ($m = 0$) (Ref. 41). Finally, at long time in the full simulation, we recover an

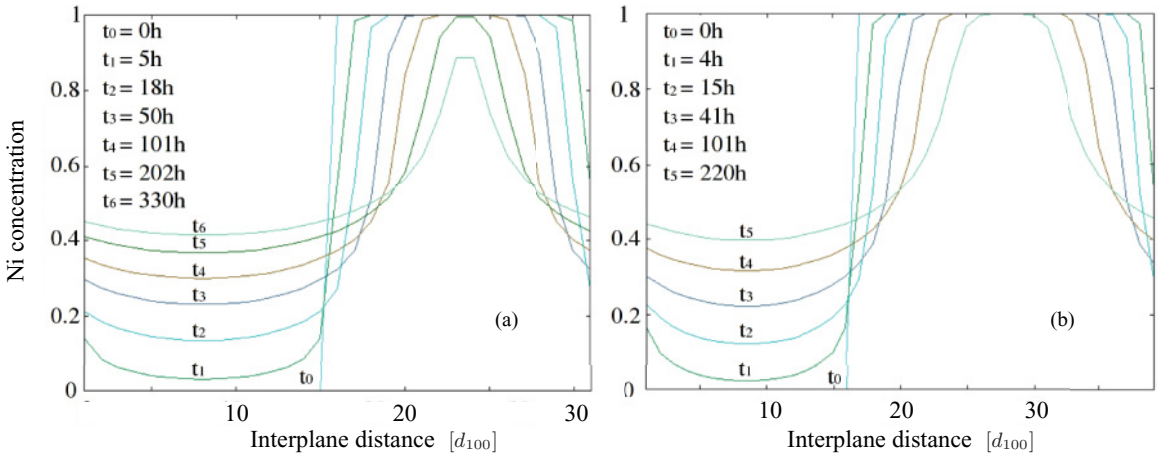

FIG. 5. (Color online) Sequence of instantaneous concentration profiles resulting from our simulations to model the kinetics in Fig. 4 for (a) *sample 1* and (b) *sample 2*.

exponential regime with a relaxation time that is controlled by the interdiffusion coefficient at the nominal concentration.

Higher order intensity peaks are even more sensitive to the interdiffusion mode and the diffusion asymmetry. This was clearly evidenced some decades ago by Fleming *et al.*[19] for semiconductor multilayer structures presenting a very low mismatch. Like in the work of Tsakalakos and Hilliard, the analysis of the diffractogram performed by Fleming *et al.* relies on the Guinier model that gives the time dependence of the amplitude of the ith harmonic of the composition modulation from the measurement of both the $I_i(t)$ and $I_{-i}(t)$ satellite peaks. Using this approach for the $(GaAs)_n(AlAs)_p$ system, Fleming *et al.* have determined a composition-dependent coefficient of the form $D(c) = D(0)\exp(-mc)$ where c is the gallium concentration.

Interestingly for the two metallic CuNi systems considered in the present paper, the presence of diffusion asymmetry can be identified from the behaviors of the satellites $I_2(t)$ and $I_{-2}(t)$. This signature appearing in the calculation of the x-ray scattered intensity is the result of a subtle interplay between the strain effect, the initial composition profile and its evolution with time in the calculation of the x-ray scattered intensity.[40] The presence of strain is necessary to observe nonidentical $I_2(t)$ and $I_{-2}(t)$ satellites. The nonsymmetrical initial composition profile is also desirable to get significant initial intensity peaks [$I_2(0)$ and $I_{-2}(0)$] on the diffraction pattern. Finally, our simulations show that for $D(c)$ constant, $I_2(t)$ and $I_{-2}(t)$ obey a similar decay while by increasing the diffusion asymmetry (by increasing m in our model) they become more and more separated with $I_{-2}(t)$ decreasing much faster than $I_2(t)$. In Fig. 4 for the two samples considered in this work, this asymmetry is clearly visible. The good qualitative agreement observed between the experiments and modeling for these particular peaks tend to confirm the prediction of the presence of a layer-by-layer interdiffusion mode in this system.

IV. CONCLUSION

We have performed x-ray diffraction experiments on coherent CuNi multilayers to probe thermoelasticity and interdiffusion in these samples. Kinetic mean-field simulations combined with the modeling of the x-ray spectra were also achieved to rationalize the experimental results. The typical coherent CuNi multilayers studied in this work have a modulation length of 6 nm and were annealed up to 640 K. At intermediate temperature in the thermoelastic regime, we first showed that the classical description based on elasticity theory remains valid to evaluate the coherency strain in these nanosized samples. This conclusion provides a valuable framework to interpret the diffractograms' evolution with time at higher temperature. Considering an interdiffusion coefficient that depends on the concentration [of the type $D(c) = D(0)\exp(-mc)$], our kinetic simulations reproduce well the time evolution of the first order and second order satellite peaks. The m values ranging from 7 to 8 while $D(0)$ is close to $1.26\ 10^{-23}\mathrm{m}^2\mathrm{s}^{-1}$ for two samples studied in detail in this work. These values are consistent with extrapolated bulk diffusion data and with the strong diffusion asymmetry expected in this system. More importantly, the resulting composition profiles and the interdiffusion mode correspond to the layer-by-layer one predicted in the past for this system.[3,16]

ACKNOWLEDGMENTS

The collaboration between Marseille and Debrecen has been supported by the PAI Balaton project "Interfaces in Nanostructures," the ERASMUS program, and the OTKA Board of Hungary (No. NF101329 and No. CK80126).

*Corresponding author: jean-marc.roussel@univ-amu.fr

[1]J. W. M. DuMond and J. P. Youtz, Phys. Rev. **48**, 703 (1935).

[2]J. W. M. DuMond and J. P. Youtz, J. Appl. Phys. **11**, 357 (1940).

[3]J.-M. Roussel and P. Bellon, Phys. Rev. B. **73**, 085403 (2006).

[4]D. B. McWhan, *Synthetic Modulated Structures* (Academic Press, New York, 1985), Chap. *Structure of Chemically Modulated Films*, p. 43.
[5]A. L. Greer and F. Spaepen, *Synthetic Modulated Structures* (Academic Press, New York, 1985), Chap. *Diffusion*, p. 419.
[6]B. J. Thaler, J. B. Ketterson, and J. E. Hilliard, Phys. Rev. Lett. **41**, 336 (1978).
[7]E. M. Gyorgy, J. F. Dillon, D. B. McWhan, L. W. Rupp, L. R. Testardi, and P. J. Flanders, Phys. Rev. Lett. **45**, 57 (1980).
[8]T. Tsakalakos and J. E. Hilliard, J. Appl. Phys. **55**, 2885 (1984).
[9]H. Barshilia and K. Rajam, Surf. Coat. Technol. **155**, 195 (2002).
[10]A. L. Greer, Curr. Opin. Solid State Mater. Sci. **2**, 300 (1997).
[11]X. Zhou, H. Wadley, R. Johnson, D. Larson, N. Tabat, A. Cerezo, A. Petford-Long, G. Smith, P. Clifton, R. Martens *et al.*, Acta Mater. **49**, 4005 (2001).
[12]Z. Balogh, M. R. Chellali, G.-H. Greiwe, G. Schmitz, and Z. Erdélyi, Appl. Phys. Lett. **99**, 181902 (2011).
[13]A. Saúl, Mater. Sci. Forum, (Trans. Tech. Publi. Switzerland) **155/156**, 233 (1994).
[14]J. M. Roussel, A. Saúl, G. Tréglia, and B. Legrand, Phys. Rev. B **60**, 13890 (1999).
[15]J.-M. Roussel, A. Saúl, G. Tréglia, and B. Legrand, Phys. Rev. B **69**, 115406 (2004).
[16]Z. Erdélyi, I. A. Szabó, and D. L. Beke, Phys. Rev. Lett. **89**, 165901 (2002).
[17]Z. Erdélyi, C. Girardeaux, Z. Tôkei, D. Beke, C. Cserháti, and A. Rolland, Surf. Sci. **496**, 129 (2002).
[18]A. Guinier, *X-Ray Diffraction: In Crystals, Imperfect Crystals, and Amorphous Bodies* (Dover, New York, 1994).
[19]R. Fleming, D. McWhan, A. Gossard, W. Wiegmann, and R. Logan, J. Appl. Phys. **51**, 357 (1980).
[20]D. Aubertine, N. Ozguven, P. McIntyre, and S. Brennan, J. Appl. Phys. **94**, 1557 (2003).
[21]N. Zotov, J. Feydt, A. Savan, and A. Ludwig, J. Appl. Phys. **100** (2006).
[22]J.-M. Roussel, S. Labat, and O. Thomas, Phys. Rev. B **79**, 014111 (2009).
[23]V. Holy, U. Pietsch, and T. Baumbach, *High Resolution X-Ray Scattering From Thin Films and Multilayers* (Springer, New York, 1999).
[24]B. R. Coles, J. Inst. Met. **84**, 346 (1956).
[25]F. Lihl, H. Ebel, A. Reichl, and A. Kaminitschek, Z. Metallkde. **59**, 735 (1968).
[26]A. K. Jena, D. Gulati, and T. R. Ramachandran, Z. Metallkd. **72**, 847 (1981).
[27]S. G. Epstein and O. N. Carlson, Acta Metal. **13**, 487 (1965).
[28]S. Brennan and P. Cowan, Rev. Sci. Instrum. **63**, 850 (1992).
[29]P. J. Brown, A. G. Fox, E. N. Maslen, M. A. O'Keefe, and B. T. M. Willis, *International Tables for Crystallography* (Kluwer Academic, Dordrecht, 1999), Vol. C, p. 551.
[30]B. E. Warren, *X-Ray Diffraction* (Addison-Wesley, Reading, MA, 1969).
[31]E. E. Fullerton, I. K. Schuller, H. Vanderstraeten, and Y. Bruynseraede, Phys. Rev. B **45**, 9292 (1992).
[32]F. Gao, Ph.D. thesis, Beijing Normal University, 2009.
[33]G. Martin, Phys. Rev. B **41**, 2279 (1990).
[34]Z. Erdélyi, G. L. Katona, and D. L. Beke, Phys. Rev. B **69**, 113407 (2004).
[35]T. B. Massalki and H. Okamoto, *Binary Alloy Phase Diagrams* (ASM International, Materials Park, OH, 1990).
[36]H. Mehrer, *Diffusion in Solid Metals and Alloys, Landolt-Börnstein, New Series*, Vol. III/26 (Springer, Berlin, 1990).
[37]V. T. Heumann and K. J. Grundhoff, Z. Metallkd. **63**, 173 (1972).
[38]Y. Iijima, K. Hirano, and M. Kikuchi, Trans. Jpn. Inst. Met. **23**, 19 (1982).
[39]J. Wang, H. S. Liu, L. B. Liu, and Z. P. Jin, Calphad **32**, 94 (2008).
[40]M.-C. Benoudia, J.-M. Roussel, S. Labat, O. Thomas, D. L. Beke, G. Langer, and M. Kis-Varga, Defect and Diffusion Forum **264**, 13 (2007).
[41]M.-C. Benoudia, Ph.D. thesis, Université Paul Cézanne Aix-Marseille, 2009.